Intelligent control of HVAC systems. Part II: perceptron performance analysis

Ioan URSU[1], Ilinca NASTASE[2]
Sorin CALUIANU[2], Andreea IFTENE*,[2], George TECUCEANU[1],
Adrian TOADER[1]

*Corresponding author
[1]INCAS – National Institute for Aerospace Research "Elie Carafoli"
B-dul Iuliu Maniu 220, Bucharest 061126, Romania
iursu@incas.ro, gtecu@incas.ro, atoader@incas.ro
*,[2] Technical University of Civil Engineering of Bucharest
Lacul Tei Bvd., no. 122-124, Bucharest 020396, Romania
ilinca.nastase@gmail.com, s_caluianu@yahoo.com, andreeaif@yahoo.com*

DOI: 10.13111/2066-8201.2013.5.3.13

Abstract: *This is the second part of a paper on intelligent type control of Heating, Ventilating, and Air-Conditioning (HVAC) systems. The whole study proposes a unified approach in the design of intelligent control for such systems, to ensure high energy efficiency and air quality improving. In the first part of the study it is considered as benchmark system a single thermal space HVAC system, for which it is assigned a mathematical model of the controlled system and a mathematical model (algorithm) of intelligent control synthesis. The conception of the intelligent control is of switching type, between a simple neural network, a perceptron, which aims to decrease (optimize) a cost index, and a fuzzy logic component, having supervisory antisaturating role for neuro-control. Based on numerical simulations, this Part II focuses on the analysis of system operation in the presence only of the neural control component. Working of the entire neuro-fuzzy system will be reported in a third part of the study.*

Key Words: *HVAC, HVAC mathematical model, HVAC intelligent control, fuzzy logic control, perceptron network, numerical simulations, perceptron network validation*.

1. INTRODUCTION

The first part of the paper [1] proposed a unified approach in the design of intelligent control for a **H**eating, **V**entilating, and **A**ir **C**onditioning (HVAC) system; Fig. 1 shows the physical model [2] which is, in fact, a benchmark system for control synthesis. The control algorithm, a fuzzy supervised neuro-control, supposed as first component a neuro-control – namely a simple perceptron (Fig. 2) – aimed at reducing the cost function

$$J = \frac{1}{2n}\sum_{i=1}^{n}\left(q_1 e_1^2(i) + e_2^2(i) + q_2 u_{nc}^2(i)\right) := \frac{1}{2n}\sum_{i=1}^{n} J(i) \tag{1}$$

where q_1, q_2 are weights on the cost function and $u := u_{nc}$ is the given neuro-control signal

$$u := u_{nc} = \nu_1 e_1 + \nu_2 e_2 \tag{2}$$

The cost function J involves a "negotiation" between the first input e_1 – the tracking error, the second input e_2 – the rate of change of tracking error, and the control u_{nc}. In fact, the procedure (2) generates two neuro-controls based on the sets of errors

$$e_{1t} := x_{1ref} - x_1, e_{2t} = \dot{e}_{1t}, e_{1h} := x_{2ref} - x_2, e_{2h} = \dot{e}_{1h} \tag{3}$$

where x_{1ref} and x_{2ref} are reference inputs. The weighting vector of the neural network, $\nu = [\nu_1\ \nu_2]^{\mathrm{T}}$, is in principle thought to be online "trained" by the gradient descent learning method to reduce the cost J

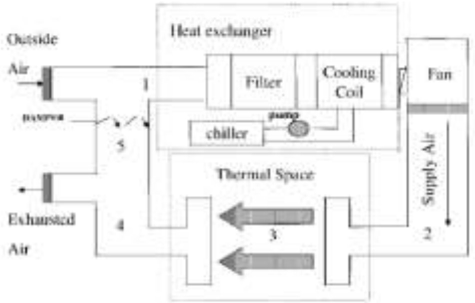

Fig. 1 – A physical model of HVAC – schematic view [2]

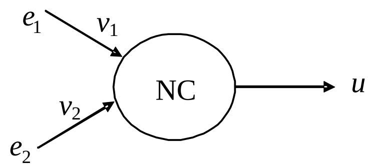

Fig. 2 − Perceptron type neuro-control

$$\boldsymbol{\nu}(n+1) = \boldsymbol{\nu}(n) + \Delta\boldsymbol{\nu}(n)$$

$$\Delta\boldsymbol{\nu}(n) := -\mathrm{diag}(\delta_1, \delta_2)\frac{\partial J}{\partial \nu(n)} = -\mathrm{diag}(\delta_1, \delta_2)\sum_{i=n-N}^{n}\left(\frac{\partial J(i)}{\partial \boldsymbol{e}(i)}\frac{\partial \boldsymbol{e}(i)}{\partial u(i)} + \frac{\partial J(i)}{\partial u(i)}\right)\frac{\partial u(i)}{\partial \boldsymbol{\nu}(i)} \tag{4}$$

In the relation (4), the matrix $\mathrm{diag}(\delta_1, \delta_2)$ introduces the learning scale vector, $\Delta\nu(n)$ is the weight vector update and N marks a back memory (of N time steps). The derivatives in (4) require only input-output information about the system. $\partial \boldsymbol{e}(i) / \partial u(i)$ is online approximated by the relationship

$$\partial \boldsymbol{e}(i) / \partial u(i) \approx (\boldsymbol{e}(i) - \boldsymbol{e}(i-1)) / (u(i) - u(i-1)) \tag{5}$$

In the absence of the physical process corresponding to physical model given in Fig. 1, the perceptron (Fig. 2) is trained on a mathematical model of the system. Recall also that the neuro-control is fuzzy logic monitored, see also [3]-[6], and this complex operation will be presented in a third part of the article.

Therefore, this is the second part of the article, aimed at analyzing the working of the system controlled by only the neural component. This objective is achieved based on numerical simulations performed on the mathematical model [1]

$$\begin{aligned}
\dot{T}_3 &= \frac{q_a}{V_3}\left(T_2 - T_3\right) - \frac{h_{wv} q_a}{c_p V_3}\left(W_2 - W_3\right) + \frac{1}{\rho c_p V_3}\left(Q - h_{wv} M\right), \dot{W}_3 = \frac{q_a}{V_3}\left(W_2 - W_3\right) + \frac{M}{\rho V_3} \\
\dot{T}_2 &= \frac{q_a\left(0.25 T_o + 0.75 T_3 - T_2\right)}{V_{he}} - \frac{q_a h_w}{c_p V_{he}}\left(0.25 W_o + 0.75 W_3 - W_2\right) - \frac{6000\mathrm{gpm}}{\rho c_p V_{he}}
\end{aligned} \tag{6}$$

This mathematical model is quite commonly used in the literature as a HVAC reference model, see [7], [8], even if raises a question mark about the dimensional coefficient 6000 gpm of the last equation. To avoid any question, it is preferable to use in simulations the system of units and the time scale of [2], as shown in the paper [9]

$$
\begin{gathered}
\dot{x}_1 = \frac{60\times\left(x_3 - x_1\right)}{58464}\times u_1 - \frac{1047.7\times 60\times\left(W_2 - x_2\right)}{0.24\times 58464}\times u_1 + \frac{\left(d_1 - 1047.7\times d_2\right)}{0.074\times 0.24\times 58464} \\
\dot{x}_2 = \frac{60}{58464}\times\left(W_2 - x_2\right)\times u_1 + \frac{d_2}{0.074\times 58464} \\
\dot{x}_3 = \frac{60}{60.75}\left(x_1 - x_3\right)\times u_1 + \frac{15}{60.75}\left(T_0 - x_1\right)\times u_1 - \\
\frac{60\times 21.78}{0.24\times 60.75}\left(0.25\times W_0 + 0.75\times x_2 - W_s\right)\times u_1 - \frac{6000}{0.24\times 0.074\times 60.75}u_2
\end{gathered}
\tag{7}
$$

Notations for system's parameters, constants and variables are: ρ − air mass density [lb/ft^3]; h_w − enthalpy of liquid water (the quantity of heat contained in 1 lb of water according to the selected temperature) [Btu/lb]; h_{wv} − enthalpy of water vapor [Btu/lb]; W_o − humidity ratio of outdoor air; W_2 − humidity ratio of supply air; $W_3(t)$ − humidity ratio of thermal space; V_{he} − volume of heat exchanger [ft^3]; c_p − specific heat of air [$\text{Btu}/\left(\text{lb}\times^\circ\text{F}\right)$]; $T_o(t)$ − temperature of outdoor air [$^\circ$F]; $T_2(t)$ − temperature of supply air [$^\circ$F]; $T_3(t)$ − temperature of thermal space [$^\circ$F]; V_3 − volume of thermal space [ft^3]; M − humidity (moisture) load [lb/hr]; Q − sensible heat load [Btu/hr]; q_a − volumetric flow rate of air [ft^3/min]; q_w − flow rate of chilled/heated water [gpm]. The enthalpies values are evaded in the reference-source of the mathematical model [2]. Given the circumstance, the values of the enthalpies were identified in order to ensure an equilibrium point as close as possible to that described in [2]. Behold such a point:

$$
\begin{gathered}
\rho = 0.074\ \text{lb/ft}^3,\ c_p = 0.24\text{Btu}/\left(\text{lb}\times^\circ\ \text{F}\right),\ u_1^e = 17000\ \text{ft}^3/\text{min},\ u_2^e = 58\ \text{gpm}, \\
x_1^e = 71\ ^\circ\text{F},\ x_2^e = 0.0092\ \text{lb/lb},\ x_3^e = 55\ ^\circ\text{F},\ d_1^e = 289843.2\ \text{Btu/hr},\ d_2^e = 166.06\ \text{lb/hr} \\
T_0^e = 85\ ^\circ\text{F},\ W_2 = 0.007\ \text{lb/lb},\ W_0^e = 0.018\ \text{lb/lb},\ V_3 = 58464\ \text{ft}^3, V_{he} = 60.75\ \text{ft}^3
\end{gathered}
\tag{8}
$$

The value chosen for the enthalpy h_{wv}, 1047.7Btu/lb, was associated to $T_0 = 85\ ^\circ\text{F}$. As for the enthalpy of liquid water h_w, to obtain a value close enough to zero for the second term of the last member of equation (7), the value $h_w = 15.797\text{Btu/lb}$ was taken. The websites referenced in [11]-[13] are useful for calculations involving the above.

2. PROTOCOL OF NUMERICAL SIMULATIONS

Let us first introduce a change of notations, as used in automatic control

$$
\begin{gathered}
x_1 := T_3, x_2 := W_3, x_3 := T_2 \\
y_1 := T_3, y_2 := W_3 \\
u_1 := q_a, u_2 := q_w \\
d_1 := Q, d_2 := M
\end{gathered}
\tag{9}
$$

i.e., for states, outputs, control and perturbations, respectively. Recall how the problem of control synthesis was posed in [1]:

Suppose that variations occur in the ambient temperature T_o*, the humidity ambient ratio* W_o*, the humidity ratio of supply air* W_2 *and the thermal loads* Q*,* M *from a certain equilibrium point* $\left(T_{\mathrm{o}}^e, W_o^e, W_2^e, Q^e, M^e\right)$ *which is in connection with a certain equilibrium state* $\left(x_1^e, x_2^e, x_3^e\right)$*. Provide an output feedback control law* $\boldsymbol{u}\left(\boldsymbol{y}(t)\right)$ *that brings the state* $\left(x_1(t), x_2(t)\right)$ *to the equilibrium point* $\left(x_1^e, x_2^e\right)$*. More specifically, the regulated (herein, measured) output* $\boldsymbol{y}(t)=\left(x_1(t) \quad x_2(t)\right)^{\mathrm{T}}$ *is required to approach the equilibrium point* $\left(x_1^e, x_2^e\right)$*.*

Therefore, to validate the effectiveness of neural control, various configurations of perturbations, of predetermined constant size, will be applied to the equilibrium (8) of the system. It will track the extent to which feedback control is able to preserve a steady state of the system, as close to the equilibrium (8). It is important to check whether this will be done with reasonable amount of control that does not exceed a saturation threshold.

3. ANALYSIS OF SIMULATION RESULTS

The control concept is as follows: the variable u_2 controls the state x_1 through state x_3, and the variable u_1 directly controls the state x_2. The mathematical model itself makes control possibilities to be atypical.

Numerical simulations of the HVAC system controlled by a neural network, of elementary perceptron type (Fig. 3), were performed using Matlab/Simulink Toolbox. The equilibrium point was considered and the system was then subjected to different configurations of perturbations $\left(T_0, W_0, d_1, d_2\right)$, summarized in Tables 1 to 5. In the Tables are shown variations of the two control values Δu_1 and Δu_2, expressed in SI units, compared to equilibrium values. Obviously, by definition, u_1 and u_2 have positive values. Equilibrium values for the control variables are $u_1^e = 17000\ \mathrm{ft}^3/\mathrm{min} = 481.38\ \mathrm{m}^3/\mathrm{min}$, and $u_2^e = 58\ \mathrm{gpm} = 0.21982\ \mathrm{m}^3/\mathrm{min}$. In simulations were considered saturation threshold values $+\Delta u_1 = 1000\ \mathrm{ft}^3/\mathrm{min} = 28.3168\ \mathrm{m}^3/\mathrm{min}$, and $+\Delta u_2 = 10\ \mathrm{gpm} = 0.0379\ \mathrm{m}^3/\mathrm{min}$.

From the results summarized in Tables we have the following findings.

a) u_2 control reacts very well to maintain reference temperature $x_1^e := T_3 = 71\ ^\circ\mathrm{F} = 21.66\ ^\circ\mathrm{C}$; for example, if the humidity W_0 increases by 10%, a decrease of 0.15% of the cooling water flow is sufficient to maintain almost unchanged the value of the reference temperature. See Fig. 3 associated with the first two rows of Table 1.

b) The perturbation of temperature of outdoor air $T_0^e = 85\ ^\circ\mathrm{F} = 29.44\ ^\circ\mathrm{C}$ by +10% requires significantly more variation of control u_2, namely +11.25%. See Fig. 4 associated with the rows 3 and 4 of Table 1.

c) As results from the mathematical model (7), the feedback control u_1 occurs only in case of a disturbance d_2. Of course, feedback control u_2 is also present, at a relatively low level of reaction. See Fig. 5 associated with the rows 5 and 6 of Table 1.

Table 1 – First set of configurations simulated on computer, with $+10\%$ perturbations

Perturbation on:	Δu_1 [ft^3/min]	Δu_2 [gpm]	d_1[Btu/hr]	d_2[lb/hr]	T_0[$^\circ$F]	W_0
W_0, cl. loop	0	-0.08723	2.898×10^5	166.1	85	0.0198
W_0, op. loop	0	0	2.898×10^5	166.1	85	0.0198
T_0, cl. loop	0	6.258	2.898×10^5	166.1	93.5	0.018
T_0, op. loop	0	0	2.898×10^5	166.1	93.5	0.018
d_2, cl. loop	0.0033	-0.05293	2.898×10^5	182.7	85	0.018
d_2, op. loop	0	0	2.898×10^5	182.7	85	0.018
d_1, cl. loop	0	4.712	3.188×10^5	166.1	85	0.018
d_1, op. loop	0	0	3.188×10^5	166.1	85	0.018
T_0,d_2, cl. loop	0.0033	6.364	2.898×10^5	182.7	93.5	0.018
T_0, d_2, op.loop	0	0	2.898×10^5	182.7	93.5	0.018
T_0, d_1, cl. loop	0	**10.97**	3.188×10^5	166.1	93.5	0.018
T_0, d_1,op. loop	0	0	3.188×10^5	166.1	93.5	0.018

Table 2 – Second set of configurations simulated on computer, with $+20\%$ perturbations

Perturbation on:	Δu_1 [ft^3/min]	Δu_2 [gpm]	d_1[Btu/hr]	d_2[lb/hr]	T_0[$^\circ$F]	W_0
W_0, cl. loop	0	-0.1745	2.898×10^5	166.1	85	0.0198
W_0, op. loop	0	0	2.898×10^5	166.1	85	0.0198
T_0, cl. loop	0	**10**	2.898×10^5	166.1	102	0.018
T_0, op. loop	0	0	2.898×10^5	166.1	102	0.018
d_2, cl. loop	0.0066	-0.06636	2.898×10^5	199.3	85	0.018
d_2, op. loop	0	0	2.898×10^5	199.3	85	0.018
d_1, cl. loop	0	**10**	3.478×10^5	166.1	85	0.018
d_1, op. loop	0	0	3.478×10^5	166.1	85	0.018
T_0, d_2, cl. loop	0.0066	**10**	2.898×10^5	199.3	102	0.018
T_0, d_2, op.loop	0	0	2.898×10^5	199.3	102	0.018
T_0, d_1, cl. loop	0	**10**	3.478×10^5	166.1	102	0.018
T_0, d_1, op. loop	0	0	3.478×10^5	166.1	102	0.018

Table 3 – Third set of configurations simulated on computer, with $+25\%$ perturbations

Perturbation on:	Δu_1 [ft^3/min]	Δu_2 [gpm]	d_1[Btu/hr]	d_2[lb/hr]	T_0[$^\circ$F]	W_0
W_0, cl. loop	0	-0.2181	2.898×10^5	166.1	85	0.0198
W_0, op. loop	0	0	2.898×10^5	166.1	85	0.0198
T_0, cl. loop	0	**10**	2.898×10^5	166.1	106.3	0.018
T_0, op. loop	0	0	2.898×10^5	166.1	106.3	0.018
d_2, cl. loop	0.00825	**10**	2.898×10^5	207.6	85	0.018
d_2, op. loop	0	0	2.898×10^5	207.6	85	0.018
d_1, cl. loop	0	**10**	3.623×10^5	166.1	85	0.018
d_1, op. loop	0	0	3.623×10^5	166.1	85	0.018
T_0, d_2, cl. loop	0.00825	**10**	2.898×10^5	207.6	106.3	0.018
T_0, d_2, op.loop	0	0	2.898×10^5	207.6	106.3	0.018
T_0, d_1, cl. loop	0	**10**	3.623×10^5	166.1	106.3	0.018
T_0, d_1, op. loop	0	0	3.623×10^5	166.1	106.3	0.018

Table 4 – Fourth set of configurations simulated on computer, with -10% perturbations

Perturbation on:	Δu_1 [ft^3/min]	Δu_2 [gpm]	d_1[Btu/hr]	d_2[lb/hr]	T_0[$^\circ$F]	W_0
W_0, cl. loop	0	0.08723	2.898×10^5	166.1	85	0.0198
W_0, op. loop	0	0	2.898×10^5	166.1	85	0.0198
T_0, cl. loop	0	-6.258	2.898×10^5	166.1	76.5	0.018
T_0, op. loop	0	0	2.898×10^5	166.1	76.5	0.018
d_2, cl. loop	-0.0033	0.03283	2.898×10^5	149.5	85	0.018
d_2, op. loop	0	0	2.898×10^5	149.5	85	0.018
d_1, cl. loop	0	-4.712	2.609×10^5	166.1	85	0.018
d_1, op. loop	0	0	2.609×10^5	166.1	85	0.018
T_0, d_2, cl. loop	-0.0033	-6.225	2.898×10^5	149.5	76.5	0.018
T_0, d_2, op.loop	0	0	2.898×10^5	149.5	76.5	0.018
T_0, d_1, cl. loop	0	-10	2.609×10^5	166.1	76.5	0.018
T_0, d_1, op. loop	0	0	2.609×10^5	166.1	76.5	0.018

Table 5 – Fifth set of configurations simulated on computer, with -20% perturbations

Perturbation on:	u_1[ft^3/min]	u_2[gpm]	d_1[Btu/hr]	d_2[lb/hr]	T_0[$^\circ$F]	W_0
W_0, cl. loop	0	0.1745	2.898×10^5	166.1	85	0.0198
W_0, op. loop	0	0	2.898×10^5	166.1	85	0.0198
T_0, cl. loop	0	-10	2.898×10^5	166.1	68	0.018
T_0, op. loop	0	0	2.898×10^5	166.1	68	0.018
d_2, cl. loop	-0.0066	0.06519	2.898×10^5	132.8	85	0.018
d_2, op. loop	0	0	2.898×10^5	132.8	85	0.018
d_1, cl. loop	0	-8.278	2.319×10^5	166.1	85	0.018
d_1, op. loop	0	0	2.319×10^5	166.1	85	0.018
T_0, d_2, cl. loop	-0.0066	-10	2.898×10^5	132.8	68	0.018
T_0, d_2, op.loop	0	0	2.898×10^5	132.8	68	0.018
T_0, d_1, cl. loop	0	-10	2.319×10^5	166.1	68	0.018
T_0, d_1, op. loop	0	0	2.319×10^5	166.1	68	0.018

We noted, however, in all configurations of Tables, outstanding efficiency of control u_1, volumetric flow rate of air, in the position of variable control for regulating the state x_2.

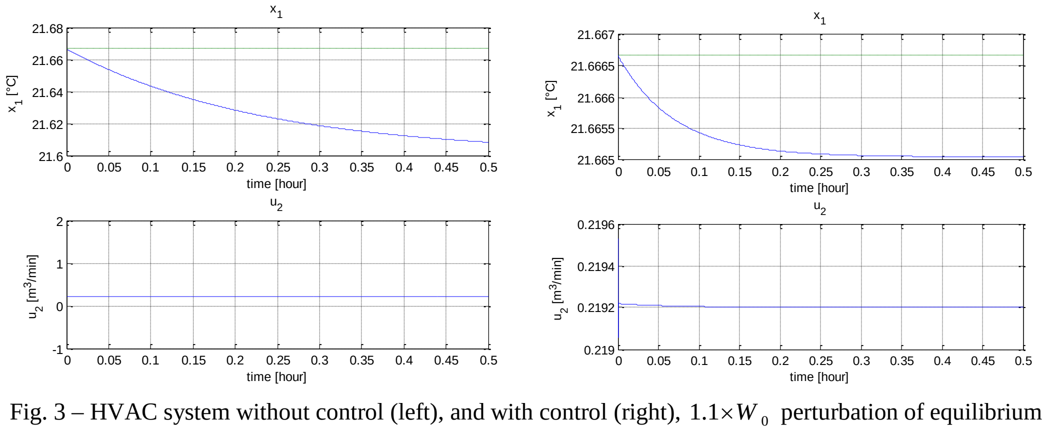

Fig. 3 – HVAC system without control (left), and with control (right), $1.1\times W_0$ perturbation of equilibrium

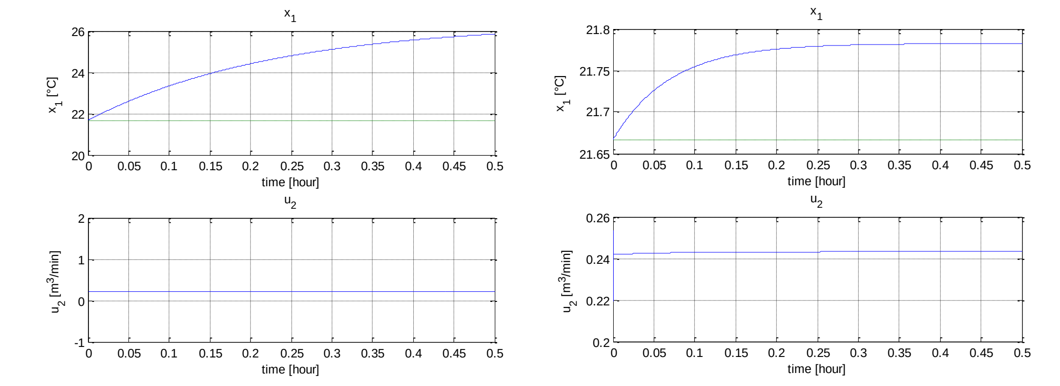

Fig. 4 – HVAC system without control (left), and with control (right), $1.1\times T_0$ perturbation of equilibrium

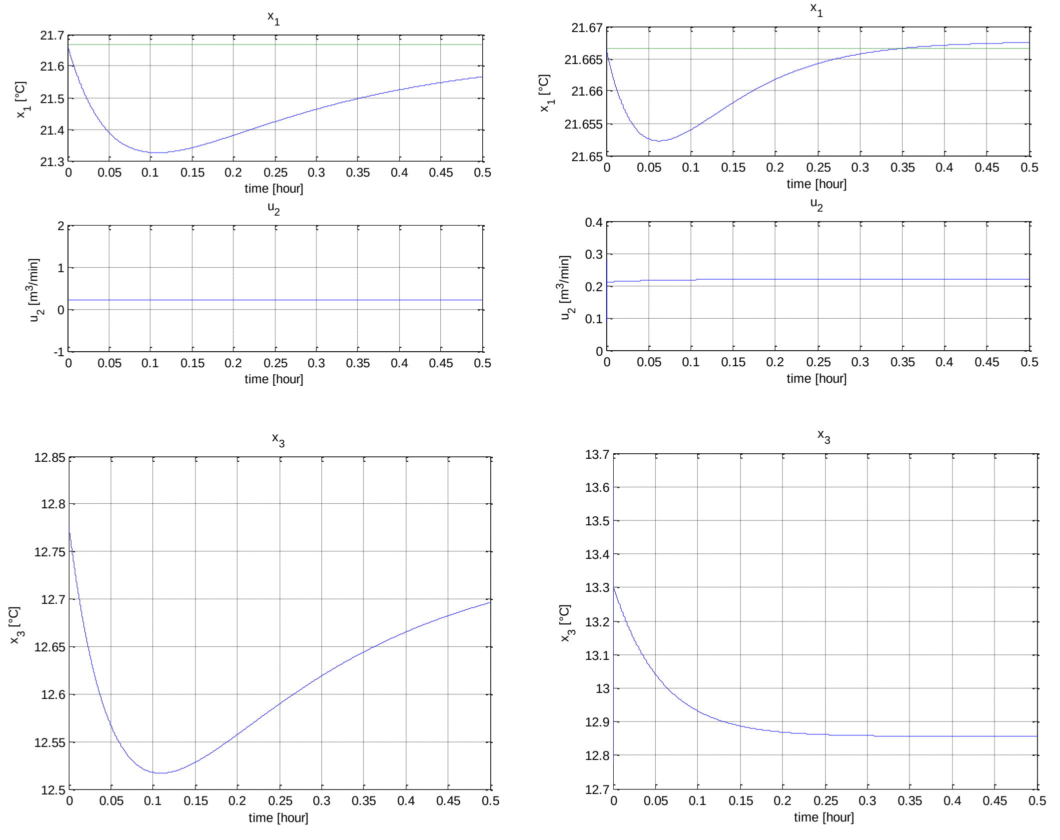

Fig. 5 – HVAC system without control (left), and with control (right), $1.1\times d_2$ perturbation of equilibrium

d) The system can not cope with any level of disturbance, as shown in Fig. 6, which is associated with the rows 5 and 6 of Table 3. It is clear that the system had saturated. The way proposed to counter such a situation is that of supervisory fuzzy logic control [1].

e) It is clear from the Tables that the sign of variations of the control variables depends on the nature of the perturbations. Thus, in Tables 1-3, in the presence of perturbations which tend to warm the thermal space, it is needed to increase the flow of cooling water, and we ascertain, for certain configurations, the occurence of the saturation (+10% threshold is introduced formal).

In Tables 4-5, the perturbations tend to cool thermal space, and the saturation appears in reverse, i.e. touching the threshold of -10%.

f) The present study is not exhaustive. Numerical simulations should continue, in view of evaluating the bounds of the perturbations that this intelligent control system can counteract, inclusively in the case of realistic presence of all the perturbations.

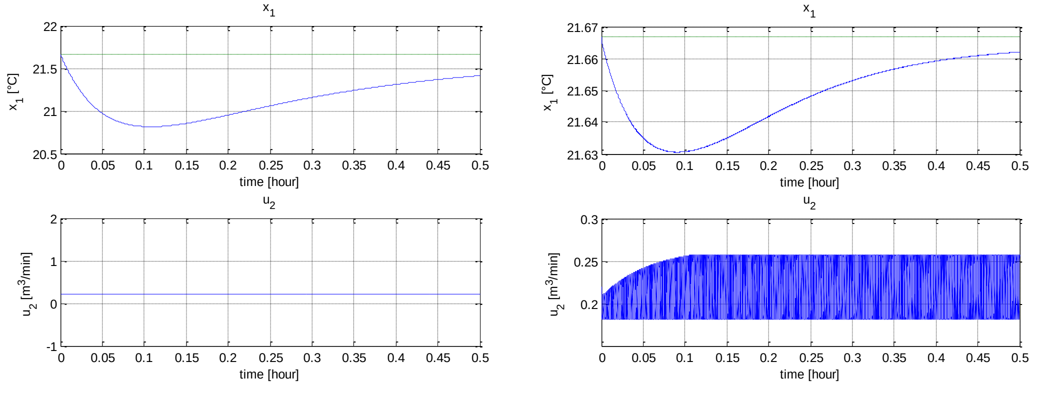

Fig. 6 – HVAC system without control (left), and with control (right), $1.25 \times d_2$ perturbation of equilibrium

5. CONCLUDING REMARKS

The mathematical model considered in this paper is one of the most commonly HVAC models referenced in literature. Therefore, it will be used in the third part of the study to validate the complete neuro-fuzzy control. It must be said that, although independent of a mathematical model of the controlled system, the intelligent control requires a careful evaluation by numerical simulations, especially with regard to the adoption of the component "rules base" of the fuzzy control. We mention also that the results of this study will serve in the development of the project [14].

The main conclusions of the numerical simulations in the paper are the following: a) the neural control can be trained to deal with a complex range of perturbations; b) the stabilization in the presence of the disturbances is achieved without the override observed with the classical control described in [2].

Acknowledgements

Some of authors gratefully acknowledge the financial support of the GRANT UEFISCDI-CNCS ROMANIA No. PN-II-PT-PCCA-2011-3.2-1212.

REFERENCES

[1] I. Ursu, I. Nastase, S. Caluianu, A. Iftene, A. Toader, Intelligent control of HVAC sysyems. Part I: Modeling and synthesis, *INCAS Bulletin*, vol. **5**, Issue 1, (online) ISSN 2247–4528, (print) ISSN 2066–8201, ISSN–L 2066–8201, DOI: 10.13111/2066-8201.2013.5.1.11, pp. 103-118, 2013.

[2] B. Argüello-Serrano, M. Velez-Reyes, Nonlinear control of a heating, ventilating and air conditioning systems with thermal load estimation, *IEEE Transaction on Control Systems Technology*, vol. **7**, no. 1, ISSN:1063-6536, pp. 56-63, 1999.

[3] I. Ursu, F. Ursu, L. Iorga, Neuro-fuzzy synthesis of flight controls electrohydraulic servo, *Aircraft Engineering and Aerospace Technology*, vol. **73**, Issue 5, ISSN: 0002-2667, pp. 465-471, 2001.

[4] I. Ursu, Felicia Ursu, *Active and semiactive control* (in Romanian), Publishing House of the Romanian Academy, 2002.

[5] I. Ursu, G. Tecuceanu, F. Ursu, R. Cristea, Neuro-fuzzy control is better than crisp control, *Acta Universitatis Apulensis*, no. 11, 259-269, 2006.

[6] I. Ursu, G. Tecuceanu, A. Toader, C. Calinoiu, Switching neuro-fuzzy control with antisaturating logic. Experimental results for hydrostatic servoactuators, *Proceedings of the Romanian Academy, Series A, Mathematics, Physics, Technical Sciences, Information Science*, **12**, 3, 231-238, 2011.

[7] E. Semsar, M. J. Yazdanpanah, C. Lucas, Nonlinear control and disturbance decoupling of an HVAC system via feedback linearization and backstepping, *IEEE Conference on Control Applications,* vol **1**, ISBN: 0-7803-7729-X, pp. 646-650, 2003.

[8] A. Parvaresh, S. M. A. Mohammadi, Adaptive self-tuning decoupled control of temperature and relative humidity for a HVAC system, *International Journal of Engineering and Science Research*, vol **2**, no. 9, ISSN 2277-2685, pp. 900-908, 2012.

[9] I. Ursu, I. Nastase, S. Caluianu, A. Iftene, A. Toader, About the synthesis and simulation of intelligent HVAC systems, *The 5th "Romanian Conference on Energy Performance of Buildings" (RCEPB-V)*, 29-30th of May, 2013, Bucharest, ROMANIA.

[10] *** *http://www.multithermcoils.com/pdf/conversion-factors.pdf*

[11] *** http://www.thermexcel.com/english/tables/eau_atm.htm and

[12] *** http://www.translatorscafe.com/cafe/EN/units-converter/fuel-efficiency-mass/5-2/

[13] *** *http://ebookbrowse.com/tablas-si-moran-shapiro-fundamentals-of-engineering-thermodynamics-5th-edition-con-r12-pdf-d419725143*

[14] *** Advanced strategies for high performance indoor Environmental QUAliTy in Operating Rooms – EQUATOR, UEFISCDI-CNCS Project No. PN-II-PT-PCCA-2011-3.2-1212.